BNL-94333-2010-BC

Ground vibration

C. Montag
Brookhaven National Laboratory

J. Rossbach
U. of Hamburg, Germany

To be published in "Handbook of Accelerator Physics and Engineering"

November 2010

Collider-Accelerator Department

Brookhaven National Laboratory

U.S. Department of Energy
Office of Science

DISCLAIMER

Ground Vibration

C. Montag, BNL
J. Rossbach, U. Hamburg

1 Basics

The variance σ^2 of a ground motion $z(t)$ (z represents transverse coordinate, either x or y) can be calculated either from its time signal or from its power spectrum $p(\omega)$,

$$\sigma^2 = \lim_{T\to\infty} \frac{1}{T} \int_{-\frac{T}{2}}^{\frac{T}{2}} z^2(t)\,\mathrm{d}t = \int_{-\infty}^{\infty} p(\omega)\,\frac{\mathrm{d}\omega}{2\pi} \tag{1}$$

with the power spectrum

$$p(\omega) = \lim_{T\to\infty} \frac{1}{T} \left| \int_{-\frac{T}{2}}^{\frac{T}{2}} z(t) \exp(-i\omega t)\,\mathrm{d}t \right|^2 . \tag{2}$$

The dimension of $p(\omega)$ is length^2/frequency.

The mutual power spectrum of two signals $z_i(t)$ and $z_j(t)$ is defined as

$$p_{ij}(\omega) = \lim_{T\to\infty} \frac{1}{T} \int_{-\frac{T}{2}}^{\frac{T}{2}} \mathrm{d}t \int_{-\frac{T}{2}}^{\frac{T}{2}} \mathrm{d}t' z_i(t') z_j(t) \exp[i\omega(t'-t)]. \tag{3}$$

The correlation (complex quantity)

$$\gamma(\omega) = \frac{\langle p_{ij}(\omega)\rangle}{\sqrt{\langle p_{ii}(\omega)\rangle \langle p_{jj}(\omega)\rangle}} \tag{4}$$

contains information on the relative phase of the motion as a function of frequency. $|\gamma(\omega)|$ is called the coherence.

For the power spectrum of relative motion of two points s_1 and s_2, separated by ΔL we get

$$\begin{aligned} \rho(\omega,\Delta L) &= \lim_{T\to\infty} \frac{1}{T} \left| \int_{-\frac{T}{2}}^{\frac{T}{2}} [(z(t,s_1) - z(t,s_2)) \exp(-i\omega t)\,\mathrm{d}t \right|^2 \\ &= p_{11}(\omega) + p_{22}(\omega) - p_{12}(\omega) - p_{21}(\omega) \end{aligned} \tag{5}$$

with variance

$$\begin{aligned} \sigma^2(\Delta L) &= \int_{-\infty}^{\infty} \rho(\omega,\Delta L)\,\frac{\mathrm{d}\omega}{2\pi} \\ &= \lim_{T\to\infty} \frac{1}{T} \int_{-\frac{T}{2}}^{\frac{T}{2}} [z_1(t) - z_2(t)]^2\,\mathrm{d}t. \end{aligned} \tag{6}$$

For the extraction of some model parameters from measured data, a 2-D power spectrum of $z(t,s)$ can be introduced [1],

$$P(\omega,k) = \lim_{T\to\infty}\lim_{L\to\infty}\frac{\left|\int_{-\frac{L}{2}}^{\frac{L}{2}}\int_{-\frac{T}{2}}^{\frac{T}{2}} z(t,s)\exp(-i\omega t - iks)\,\mathrm{d}t\,\mathrm{d}s\right|^2}{TL} \tag{7}$$

with

$$p(\omega) = \int_{-\infty}^{\infty} P(\omega,k)\,\frac{\mathrm{d}k}{2\pi} \tag{8}$$

$$\rho(\omega,\Delta L) = \int_{-\infty}^{\infty} P(\omega,k)\cdot 2[1-\cos(k\Delta L)]\,\frac{\mathrm{d}k}{2\pi}. \tag{9}$$

Therefore,

$$\sigma^2 = \int_{-\infty}^{\infty}\int_{-\infty}^{\infty} P(\omega,k)\,\frac{\mathrm{d}\omega}{2\pi}\,\frac{\mathrm{d}k}{2\pi} \tag{10}$$

$$\sigma^2(\Delta T,\Delta L) = \int_{-\infty}^{\infty}\int_{-\infty}^{\infty}\frac{\mathrm{d}\omega}{2\pi}\,\frac{\mathrm{d}k}{2\pi}P(\omega,k) \cdot 2[1-\cos(\omega\Delta T)]\cdot 2[1-\cos(k\Delta L)]. \tag{11}$$

A useful model of the uncorrelated part of ground motion is given by the ATL rule [2]:
The variance σ^2 of the uncorrelated motion of two points separated by ΔL, observed after a time interval ΔT (assuming $z_1 - z_2 = 0$ at $t = 0$) is proportional to the distance ΔL and the time interval ΔT,

$$\sigma^2(\Delta T,\Delta L) = A\cdot\Delta T\cdot\Delta L \tag{12}$$

with corresponding power spectrum

$$\rho(\omega,\Delta L) = \frac{A\cdot\Delta L}{\omega^2}. \tag{13}$$

ATL-like motion has been confirmed in numerous measurements of ground motion [3] and beam orbits in accelerators [4].

2 Measurements

Since measured data consist of real numbers only, there is no additional information from negative frequencies: $p(\omega) = p(-\omega)$. Thus a slightly different definition of the power spectrum is useful:

$$p(\omega) = \lim_{T\to\infty}\frac{2}{T}\left|\int_{-\frac{T}{2}}^{\frac{T}{2}} z(t)\exp(-i\omega t)\,\mathrm{d}t\right|^2 \tag{14}$$

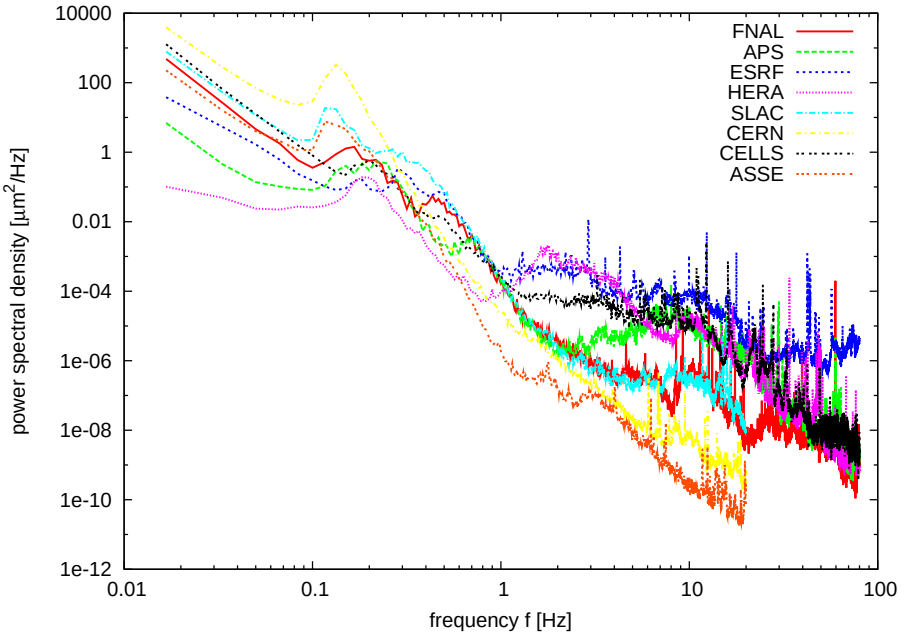

Figure 1: Example of power spectra measured at several accelerator sites [5]. An additional reference curve was taken at ASSE, a former German salt mine, about 900 m below sea level (National Datum Level −900 m).

with

$$\sigma^2 = \int_0^\infty p(\omega)\,\frac{\mathrm{d}\omega}{2\pi}, \tag{15}$$

i.e. $p(\omega)$ is defined for positive frequencies only.

The rms-value in the frequency band f_0 to f_1 can be calculated by integrating the power spectrum over this frequency band:

$$\sigma(f_0 < f < f_1) = \sqrt{\int_{2\pi f_0}^{2\pi f_1} p(\omega)\,\frac{\mathrm{d}\omega}{2\pi}}. \tag{16}$$

Using the coherence $|\gamma(\omega)|$, the ratio $\beta(\omega)$ of correlated to uncorrelated ground motion can be computed as

$$\beta(\omega) = \frac{|\gamma(\omega)|^2}{1-|\gamma(\omega)|^2}. \tag{17}$$

For a compilation of vertical ground motion spectra at various accelerator sites, see Fig.1 [5].

Characteristics of all spectra:

- Microseismic peak around 1/7 Hz, caused by ocean waves hitting coasts (the "7-second hum").
- Broad peak around 2.5 Hz. Its origin is explained by either some band-pass characteristics of the ground surface or as a result of cultural noise and damping both increasing with frequency, but with damping becoming effective at slightly higher frequencies.
- cultural noise beyond ≈ 5 Hz, caused by traffic, heavy machinery, etc.

3 Instruments

3.1 Piezoelectric accelerometers

A piezo crystal is mounted to the sensor housing from one side; the other side is loaded with a seismic mass. Therefore, the crystal acts as a kind of spring which is sheared when the sensor is accelerated in its sensitive direction. Below the mechanical resonance frequency (usually several kHz), the output charge C is proportional to the acceleration $a = \mathrm{d}^2 z/\mathrm{d}t^2$. Since the charge amplifier is sensitive to a charge change $\dot{C} = \mathrm{d}C/\mathrm{d}t$, three integrations are necessary to obtain the displacement z. This results in a rather high noise level at low frequencies.

3.2 Geophones and seismometers

Geophones basically consist of a coils suspended from a spring within the field of a permanent magnet. The voltage induced in the coil is proportional to the velocity of the coil with respect to the spring. Above the mechanical resonance frequency of typically 1 Hz, this velocity equals the instantaneous velocity of the instrument housing with respect to an inertial system. To obtain the displacement, the output signal has to be integrated once.

In a seismometer, this purely passive arrangement is equipped with a PI feedback system which is designed such as to modify the mechanical transfer function of the instrument, thus resulting in a transfer function equal to that of a resonator with a resonance frequency of typical several 10^{-3} Hz.

3.3 Hydrostatic level sensors

Hydrostatic level sensors employ capacitive sensors to monitor water levels in a system of communicating tubes. Local water temperature meters are added to compensate for thermal expansion. These sensors are ideally suited for the study of spatial diffusion and correlation of ground motion.

4 Linacs

The rms beam displacement σ_z at the end of a linac due to random misalignment of all N_q quadrupoles with equal focal length f is given by

$$\sigma_z^2 = \sum_{N_q} \frac{\gamma_q}{\gamma_{\rm end}} \overline{\beta}\, \overline{\beta}_{\rm end} \frac{1}{2} \frac{\sigma_q^2}{f^2}, \tag{18}$$

with $\overline{\beta}$ the β-function averaged over a FODO cell of length $L_{\rm FODO}$, and the Lorentz factor γ. In a linac with periodic FODO lattice and β-function scaling $\beta \propto \gamma^n$, the rms beam jitter σ_z due to uncorrelated rms quadrupole jitter σ_q is

$$\sigma_z^2 = \sigma_q^2 \overline{\beta}_{\rm end}^2 \int \frac{1}{f^2} \left(\frac{\gamma}{\gamma_{\rm end}} \right)^{n+1} \frac{{\rm d}s}{L_{\rm FODO}}, \tag{19}$$

where the sum has been replaced by an integral, while $2/L_{\rm FODO}$ is the local line density of quadrupoles.

With ${\rm d}s = L_{\rm tot} {\rm d}(\gamma/\gamma_{\rm end})$, $1/f = (4/L)\sin(\mu/2)$ and $\overline{\beta} = L/\sin\mu$ we get under the assumption of a constant phase advance μ per FODO cell and for $n < 0.8$:

$$\sigma_z^2 \approx \frac{4\sigma_q^2 L_{\rm tot}}{\overline{\beta}_{\rm end} \sin\mu \cos^2\frac{\mu}{2}} \frac{1}{2-2n}, \tag{20}$$

where $L_{\rm tot}$ is the linac length. With

$$N_q = \frac{2L_{\rm tot}}{\langle L_{\rm FODO} \rangle} \approx \frac{2L_{\rm tot}}{(1-n)\overline{\beta}_{\rm end} \sin\mu} \tag{21}$$

the rms beam jitter at the end of the linac is [6]

$$\sigma_z = \frac{\sigma_q \sqrt{N_q}}{\cos\frac{\mu}{2}}. \tag{22}$$

This beam motion can lead to emittance growth due to wakefield excitation [7] and to luminosity loss in colliding beam facilities.

If both beams of beam size $\sigma_{\rm beam}$ jitter independently with rms-value σ_z, this results in a luminosity degradation according to

$$\mathcal{L} = \mathcal{L}_0 \exp\left(-2 \frac{\sigma_z^2}{4\sigma_{\rm beam}^2} \right). \tag{23}$$

In a periodic FODO lattice with $\beta \propto \sqrt{\gamma}$, the uncorrelated quadrupole jitter tolerance can therefore be estimated at [6]

$$\sigma_q \quad = \quad \sqrt{\frac{\sigma_z^2}{N_q}} \cos\frac{\mu}{2}$$

$$= \sqrt{\frac{-2\sigma_{\rm beam}^2 \ln\frac{\mathcal{L}}{\mathcal{L}_0}}{N_q}}\cos\frac{\mu}{2}$$
$$= \sqrt{\frac{-2\epsilon_{\rm end}\overline{\beta}_{\rm end} \ln\frac{\mathcal{L}}{\mathcal{L}_0}}{N_q}}\cos\frac{\mu}{2}, \quad (24)$$

with $\epsilon_{\rm end}$, $\overline{\beta}_{\rm end}$, N_q, and μ being the geometric emittance at the end of the main linac, the average β-function of the last FODO cell, the number of quadrupoles per linac, and the phase advance per FODO cell, respectively.

Next we assume a single plane wave travelling at an angle Θ_w to the linac,

$$z_{\rm gr}(s) = \hat{z}_{\rm gr}\cos[k_{\rm gr}s\cos\Theta_w + \phi_0], \quad (25)$$

with s and ϕ_0 being the longitudinal coordinate and the wave phase, respectively. $k_{\rm gr}$ is the wave number of the ground motion wave. The response $\Delta z_{\rm end}(L)$ of the central trajectory at the end of the linac can be calculated as

$$\Delta z_{\rm end}(L) = \int_0^L K_1(s) z_{\rm gr}(s) R_{12}(s,L)\,{\rm d}s. \quad (26)$$

Here $K_1(s)$ is the quadrupole strength at position s, $R_{12}(s,L)$ is the (1,2)-element of the transfer matrix from s to the end of the linac, L. Assuming $\beta \propto \sqrt{\gamma}$, $K_1 \propto 1/\gamma$, and the lengths of drift spaces and quadrupoles $L_q \propto \sqrt{\gamma}$, we can write [6]

$$\begin{aligned}\Delta z_{\rm end}(L) &= (K_1 L_q)_0 \hat{z}_{\rm gr}\sqrt{\frac{\gamma_0}{\gamma_f}}\sqrt{\beta_f}\sum_{n=0}^{N_q-1}\left(\frac{\gamma_n}{\gamma_0}\right)^{1/4} \\ &\quad\cdot\cos(k_{\rm gr}s_n\cos\Theta_w + \phi_0) \\ &\quad\cdot\sqrt{\beta_0}\sin(\mu_f - n\mu/2)\frac{K_1}{|K_1|}. \end{aligned} \quad (27)$$

Here s_n and γ_n are the position and energy at the nth quadrupole, while $K_1/|K_1|$ changes sign for focusing and defocusing quadrupoles.

Time averaging yields [6]

$$\begin{aligned}\sigma_z^2 &= (K_1 L_q)_0^2 \frac{\hat{z}_{\rm gr}^2}{8}\frac{\gamma_0}{\gamma_f}\beta_f \\ &\quad\cdot\left|\sum_{\pm}\sum_{n=0}^{N_{\rm cell}-1}\left(\frac{\gamma_n}{\gamma_0}\right)^{1/4}\exp[i(k_{\rm gr}\cos\Theta_w)s_n \pm n\mu]\right. \\ &\quad\cdot\left.\left(\sqrt{\hat{\beta}_0} - \sqrt{\check{\beta}_0}\exp[i(k_{\rm gr}\cos\Theta_w L_n/2 \pm \mu/2)]\right)\right|^2, \end{aligned} \quad (28)$$

where $\hat{\beta}_0$ and $\check{\beta}_0$ are the initial maximum and minimum β-functions, $N_{\rm cell}$ is the number of FODO cells, L_n the length of the nth cell, and the sum over $\pm$ is the sum over both the sum phase and the difference phase.

Equation 28 becomes resonant when

$$k_{\rm gr} L_c \pm \mu = 2\pi p, \;\; p \text{ integer.} \tag{29}$$

With the scalings mentioned above, $\sigma_z^2 = \langle z_c^2 \rangle$ becomes [6]

$$\begin{aligned} \langle z_c^2 \rangle &\approx \frac{\pi N_q \tan \mu/2}{2L_0^3} \frac{\gamma_0}{\gamma_f} \left(\frac{z_{\rm gr}}{k_{\rm gr} \cos \Theta_w} \right)^2 \\ &\cdot \sum_{\rm resonances} (2\pi p \pm \mu) \left(\sqrt{\hat{\beta}_0} - (-1)^p \sqrt{\check{\beta}_0} \right)^2 . \end{aligned} \tag{30}$$

The assumption of correlated quadrupole motion tends to be appropriate at low frequencies. At high frequencies ground motion is uncorrelated even for short distances of a few meters and no longer wave-like.

5 Circular Accelerators

For uncorrelated misalignment of quadrupoles in a periodic lattice, the rms closed orbit distortion $\sigma_{\rm co}(s)$ at an azimuthal position s is

$$\sigma_{\rm co} = \frac{\sqrt{\beta(s)}\sqrt{\langle\beta\rangle}}{2 \sin \pi\nu} \frac{\sigma_q}{|f|} \sqrt{N}, \tag{31}$$

with betatron tune ν, focal length f, transverse rms quadrupole misalignment σ_q and number N of identical FODO cells. The average $\langle\beta\rangle$ is taken at the quadrupoles.

Consider a storage ring of circumference $C = 2\pi R$ which is composed of N identical FODO cells and identical bends between the quads. The betatron phase advance per FODO cell is μ, so the tune of the ring is $\nu = n\mu/2\pi$.

5.1 Vertical orbit distortion due to a single vertical ground wave

Motion of the nth qudrupole at azimuthal angle Θ_n, measured with respect to the observation point at $\Theta = 0$, due to a ground wave with amplitude $\hat{y}$, phase ϕ_0 with respect to the ring center, frequency $\omega/2\pi$, velocity v, wavelength $\lambda = v/(\omega/2\pi)$, and direction of incidence Θ_w :

$$\Delta y_n(t) = \hat{y} \Re \exp \left\{ i \left[\omega t + \frac{\omega R}{v} \cos(\Theta_n - \Theta_w) + \phi_0 \right] \right\}. \tag{32}$$

The closed orbit distortion at the observation point with β-function β_0 due to Δy_n is

$$y_c = \Re \left\{ \frac{\sqrt{\beta_0}}{2 \sin \pi\nu_y} \frac{\hat{y}}{f} \exp[i(\omega t + \phi_0)] \right.$$

$$\cdot \left[\sum_{n=2}^{2N} \sqrt{\hat{\beta}} \exp[i(C/\lambda)\cos(\Phi_n/\nu_y - \Theta_w)] \cos(\Phi_n - \pi\nu_y) \right.$$
$$\left. - \sum_{n=1}^{2N-1} \sqrt{\check{\beta}} \exp[i(C/\lambda)\cos(\Phi_n/\nu_y - \Theta_w)] \cos(\Phi_n - \pi\nu_y) \right] \Bigg\}. \quad (33)$$

Here, Φ_n and $\beta_{y,n}$ are the (vertical) betatron phase advance between the observation point and the nth magnet, and the vertical β-function at the nth magnet, respectively. $\hat{\beta}$ and $\check{\beta}$ are the β-functions at focusing and defocusing quads. The response R_y, i.e. the ratio of the closed-orbit distortion $\hat{y}_c$ divided by the amplitude $\hat{y}$ of the plane ground wave, is [8, 9]

$$\begin{aligned} R_y &= \frac{\hat{y}_c}{\hat{y}} \\ &= \frac{\sqrt{\beta_0}}{2f} \left\{ \left[\sum_{p=-\infty}^{\infty} J_{4p}\left(\frac{C}{\lambda}\right) C_{4p} - J_{4p-2}\left(\frac{C}{\lambda}\right) C_{4p-2} \right]^2 \right. \\ &\quad \left. + \left[\sum_{p=-\infty}^{\infty} J_{4p-1}\left(\frac{C}{\lambda}\right) C_{4p-1} - J_{4p-3}\left(\frac{C}{\lambda}\right) C_{4p-3} \right]^2 \right\}^{\frac{1}{2}}, \quad (34) \end{aligned}$$

with J_p the Bessel function and

$$\begin{aligned} C_p &= \frac{(-1)^{p+1}}{\sin\left(\frac{\pi p}{N} - \frac{\mu}{2}\right)} \\ &\quad \cdot \left\{ \sqrt{\hat{\beta}} \cos\left[p\left(\pi \frac{N+1}{N} - \Theta_w \right) - \frac{\mu}{2} \right] \right. \\ &\quad \left. - \sqrt{\check{\beta}} \cos[p(\pi - \Theta_w)] \right\}. \quad (35) \end{aligned}$$

C_p becomes resonant for

$$|p| = |m|N \pm \nu_y. \quad (36)$$

With $\delta\nu_y$ the distance of ν_y from the closest integer $[\nu_y]$, the maxima of the resonance term

$$\left| \sin\left(\frac{\pi p}{N} - \frac{\Delta\Phi}{2} \right) \right|^{-1} \quad (37)$$

can be expressed as

$$\frac{1}{\sin \frac{\pi}{N}\delta\nu_y}, \quad (38)$$

occuring whenever

$$p_{\text{res}} = mN + [\nu_y]. \quad (39)$$

The Bessel function J_p in Eq.34 differs significantly from zero only for arguments $C/\lambda > p$. Since all contributions with $p \neq p_{\rm res}$ are suppressed, ground waves with $C/\lambda > p_{\rm res}$ contribute much more to R_y than those with smaller C/λ (see Fig.2). Thus, R_y is small for small C/λ and rises in a step-like manner at $C/\lambda = [\nu_y], N - [\nu_y], N + [\nu_y], 2N - [\nu_y]$, etc. [9].

5.2 Horizontal orbit distortion due to a single incident plane ground wave

Horizontal waves move the magnets not only in the transverse direction, but also longitudinally, i.e. in the direction along the closed orbit. The amount of this longitudinal motion depends on the difference between the azimuthal position Θ_n of the magnet and the direction of incidence Θ_w. The horizontal motion of the nth quadrupole is

$$\begin{aligned} \Delta x_n(t) &= \hat{x}\cos(\Theta_n - \Theta_w) \\ &\quad \cdot \Re \exp\left\{ i \left[\omega t + \frac{C}{\lambda}\cos(\Theta_n - \Theta_w) - \phi_0 \right] \right\}. \end{aligned} \tag{40}$$

For the response function we get

$$\begin{aligned} R_x &= \frac{\hat{x}_c}{\hat{x}} \\ &= \frac{\sqrt{\beta_0}}{2f} \left\{ \left[\sum_{p=-\infty}^{\infty} J'_{4p}\left(\frac{C}{\lambda}\right) C_{4p} - J'_{4p-2}\left(\frac{C}{\lambda}\right) C_{4p-2} \right]^2 \right. \\ &\quad \left. + \left[\sum_{p=-\infty}^{\infty} J'_{4p-1}\left(\frac{C}{\lambda}\right) C_{4p-1} - J'_{4p-3}\left(\frac{C}{\lambda}\right) C_{4p-3} \right]^2 \right\}^{\frac{1}{2}}, \end{aligned} \tag{41}$$

which is identical to that in the vertical case, except for replacing J_p by its derivative J'_p.

As in the case of vertical quadrupole motion, resonances occur for

$$|p| = |m|N \pm [\nu_x], \tag{42}$$

i.e. with increasing C/λ the response behaves in a way similar to R_y.

5.3 Vertical orbit distortion due to an ensemble of plane ground waves

Consider a large number M of plane ground waves of equal frequency $\omega/2\pi$ and equal wavelength λ, incident from arbitrary directions Θ_m with phases ϕ_m and amplitudes $\hat{y}_m$. The vertical motion of the nth quadrupole is

$$\Delta y_n(t) = \sum_{m=1}^{M} \hat{y}_m$$

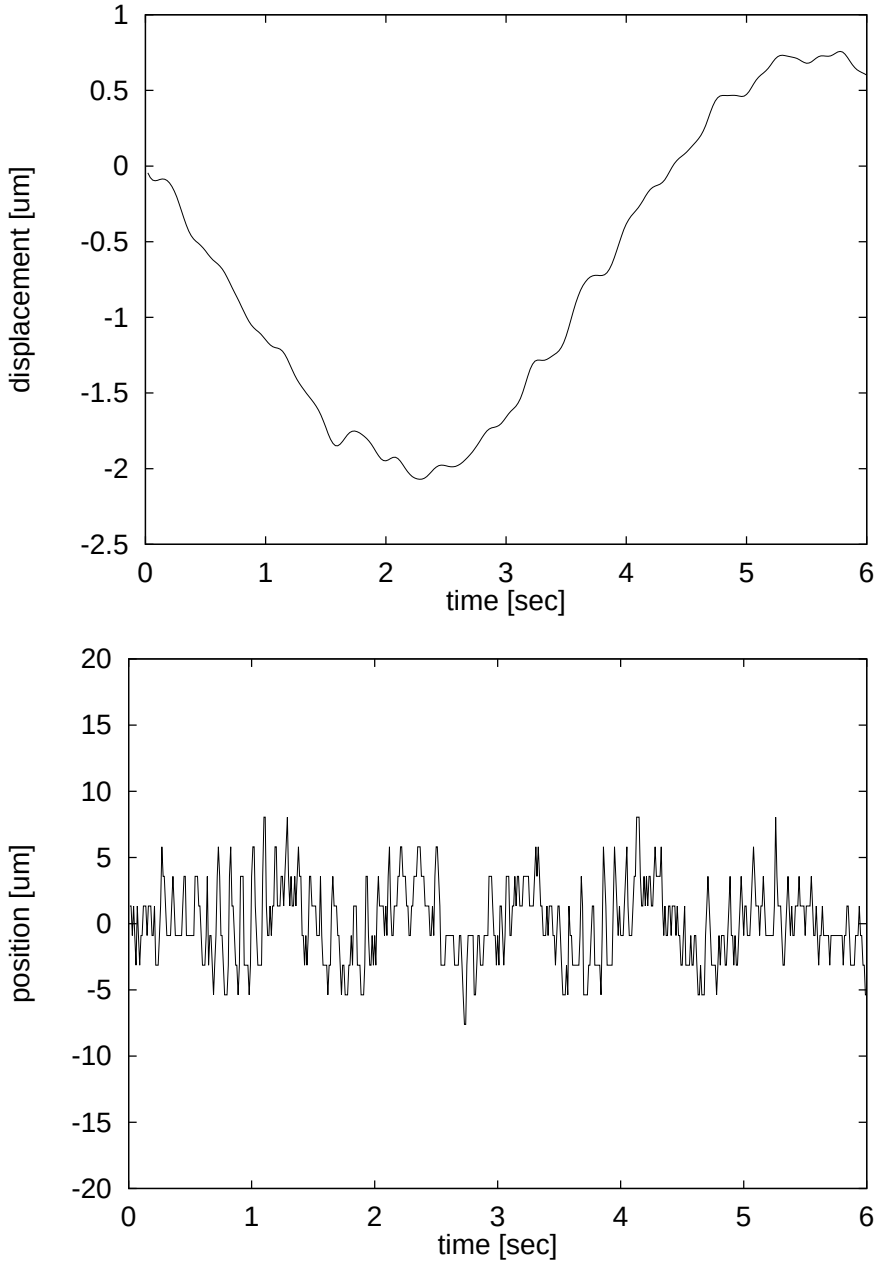

Figure 2: Example of ground motion (upper) and beam vibration (lower), normalized to $\beta = 1\,\mathrm{m}$. As expected, the low frequency part of ground motion (the microseismic peak around $1/7\,\mathrm{Hz}$) is not present in the beam motion due to its long wavelength.

$$\cdot \Re \exp\left\{ i \left[\omega t + \frac{C}{\lambda} \cos(\Theta_n - \Theta_m) + \phi_m \right] \right\}. \tag{43}$$

The rms response $R_y^{\rm rms}$ yields [9]

$$\begin{aligned} R_y^{\rm rms} &= \frac{\text{rms closed} - \text{orbit distortion}}{\text{rms ground motion}} \\ &= \frac{\sqrt{\beta_0}}{2f} \left\{ J_0^2\left(\frac{C}{\lambda}\right) \left(\frac{\sqrt{\hat\beta}\cos\frac{\mu}{2} - \sqrt{\check\beta}}{\sin^2\frac{\mu}{2}} \right)^2 \right. \\ &\quad + \sum_{p=1}^{\infty} J_p^2\left(\frac{C}{\lambda}\right) \left[\frac{\hat\beta + \check\beta - 2\sqrt{\hat\beta\check\beta}\cos\left(\frac{p\pi}{N} - \frac{\mu}{2}\right)}{2\sin^2\left(\frac{p\pi}{N} - \frac{\mu}{2}\right)} \right. \\ &\quad + \frac{\hat\beta + \check\beta - 2\sqrt{\hat\beta\check\beta}\cos\left(\frac{p\pi}{N} + \frac{\mu}{2}\right)}{2\sin^2\left(\frac{p\pi}{N} + \frac{\mu}{2}\right)} \\ &\quad \left. \left. + 2\frac{\hat\beta\cos\mu + \check\beta - 2\sqrt{\hat\beta\check\beta}\cos\frac{\mu}{2}\cos\frac{p\pi}{N}}{\cos\frac{2\pi p}{N} - \cos\mu} \right] \right\}^{\frac{1}{2}} \end{aligned} \tag{44}$$

5.4 Horizontal orbit distortion due to an ensemble of plane ground waves

The response to a horizontal compression wave can be described by the same equations as for the vertical case if one just replaces J_p by J_p' and uses the appropriate horizontal optics parameters. One must not forget an additional factor $\sqrt{2}$ arising from averaging $\cos^2(\Theta - \Theta_m)$ when computing the rms value,

$$\langle [\Delta x_n(t)]^2 \rangle^{\frac{1}{2}} = \left(\frac{1}{4} \sum_m \langle \hat{x}_m^2 \rangle \right)^{\frac{1}{2}}. \tag{45}$$

6 Numerical modeling

While numerical modeling of ground motion in linacs is straightforward [10], simulation of ATL-like motion in circular accelerators is more involved [11].

According to the ATL model, the (vertical) position Y_i relative to a (conceptual) fixed reference point 0 after time T is given as

$$\langle Y_i^2 \rangle = ATL_{i0}, \tag{46}$$

where L_{i0} denotes the distance of location i from the fixed reference point.

From the relative motion of two locations i and j

$$\langle (Y_i - Y_j)^2 \rangle = \langle Y_i^2 \rangle + \langle Y_j^2 \rangle - 2\langle Y_i Y_j \rangle \tag{47}$$

it then follows that

$$\langle Y_i Y_j \rangle = AT\frac{1}{2}(L_{i0} + L_{j0} - L_{ij}) = AT M_{ij}, \tag{48}$$

or in matrix notation,

$$\langle \vec{Y} \cdot \vec{Y}^T \rangle = AT\mathbf{M}. \tag{49}$$

$\mathbf{M}$ is symmetric and can be diagonalized by a unitary matrix Λ,

$$\tilde{\mathbf{M}} = \Lambda \cdot \mathbf{M} \cdot \Lambda^T, \tag{50}$$

with the components of $\tilde{\mathbf{M}}$ being the eigenvalues λ_i of $\mathbf{M}$,

$$\tilde{M}_{ij} = \lambda_i \delta_{ij}. \tag{51}$$

An appropriate choice of the reference point 0 ensures that $\tilde{\mathbf{M}}$ is diagonal.

Defining the vector $\vec{V}$ as

$$\vec{V} = \Lambda \cdot \vec{Y} \tag{52}$$

and premultiplying Eq.49 by Λ and postmultiplying it by Λ^T yields the result

$$\begin{aligned} \langle \vec{V}\vec{V}^T \rangle &= \Lambda \langle \vec{Y}\vec{Y}^T \rangle \Lambda^T = AT\tilde{\mathrm{M}} \\ &\Rightarrow \langle V_i^2 \rangle = AT\lambda_i. \end{aligned} \tag{53}$$

Explicitly, we construct the symmetric matrix $\mathbf{M}$ from the distances between the various locations under consideration and a chosen fixed reference point, and find its eigensystem. Then we generate a set of values with variances given by the eigenvalues of $\mathbf{M}$, and transform these values using the eigenvectors of $\mathbf{M}$ to find the corresponding vertical displacements.

References

[1] A. Sery, O. Napoly, PRE 53 (1996)

[2] B. Baklakov et al., Sov. Phys. Zh TF.63 (1993) 10 (in Russian)

[3] V. Shiltsev, PRL 104, 238501 (2010)

[4] R. Brinkmann and J. Rossbach, NIM A 350 (1994) 8-12

[5] W. Bialowons, J. A. Osborne, and G. Shirkov, ILC-HiGrade-Report-2010-004-1

[6] T. Raubenheimer, SLAC-387 (1991)

[7] M. Drevlak, DESY 95-225

[8] T. Aniel, J. L. Laclare, LNS/086 Saclay (1985)

[9] J. Rossbach, PA 23 (1988) 121

[10] C. Montag, DESY 97-030

[11] A. Wolski and N. J. Walker, Proc. PAC 2003, 2396-2398 (2003)